Polymer 208 (2020) 122880

Contents lists available at ScienceDirect

Polymer

journal homepage: http://www.elsevier.com/locate/polymer

Hierarchical self-assembly of supramolecular polymer complexes mediated by various generations of bent-core mesogenic dendrimers hydrogen-bonded with triblock copolymer

Chien-Min Lin [a], Atul Kumar Dwivedi [a], Wei-Tsung Chuang [b,c,**], Hong-Cheu Lin [a,d,*]

[a] Department of Materials Science and Engineering, National Chiao Tung University, Hsinchu, 30049, Taiwan
[b] National Synchrotron Radiation Research Center, Hsinchu, 30076, Taiwan
[c] Graduate Institute of Applied Science and Technology, National Taiwan University of Science and Technology, Taipei, 106335, Taiwan
[d] Center for Emergent Functional Matter Science, National Chiao Tung University, Hsinchu, 30049, Taiwan

ARTICLE INFO

Keywords:
Block copolymer
Hydrogen-bonded
Dendritic proton donor

ABSTRACT

A series of side-chain supramolecular polymer complexes containing proton acceptor triblock copolymer, i.e., poly(4-vinylpyridine)-block-polystyrene-block-poly(4-vinylpyridine) (**VSV**, i.e., P4VP-PS-P4VP), hydrogen-bonded (H-bonded) with two generations of proton donor bent-core mesogenic dendritic pendants (**G1** and **G2**) were prepared and investigated. These two supramolecular polymer complexes (i.e., **VSV/G1** and **VSV/G2**) were characterized by wide- and small-angle X-ray scattering (WAXS and SAXS), and the formation of a microphase separated smectic A (SmA) structure corresponding to a head-to-head layered arrangement was confirmed. The hierarchical structures within the morphologies of supramolecular polymer complexes were proved not only by the SAXS patterns but also by the transmission electron microscopy (TEM). The novel hierarchical lamellar domains of corresponding tetragonal and hexagonal arrangements in different generations of dendritic proton donors (**G1** and **G2**) were self-assembled with triblock copolymer proton acceptor **VSV** to induce respective BCC (body-centered cubic) and FCC (face-centered cubic) structures in supramolecular polymer complexes **VSV/G1** and **VSV/G2**. Therefore, the shear alignments of characteristic cylindrical column phase micro-domains were developed for the first time to control the unique hierarchical constructions of functionalized self-assembled bent-core structures by utilization of various generations of dendritic proton donors to be H-bonded with triblock copolymer proton acceptor.

1. Introduction

The remarkable utilities of block copolymers (BCPs) as the building blocks of nanomaterials have been witnessed for a few past decades [1,2], including incompatibilities within different BCPs offering various morphologies on the base of various volume fractions of individual blocks [3–5]. On the other hand, dendrimers with their three dimensional and highly branched structures consisting of a large number of end groups possess unique properties in contrast to those linear polymers. Therefore, dendrimers with various end group functionalities are highly demanded for many applications in materials science [6–9]. Therefore, Mezzenga et al. reported a series of dendrons, dendrimers, and side-chain dendronized polymers which were systematically complexed with one-three generations of dendritic units [10]. The structural properties and geometries of lamellar, columnar hexagonal, oblique columnar, and rectangular columnar phases were found to be dependent on the types and generations of dendritic molecules. These results explain the direct correlation among the degrees of freedom and orders of the dendritic macromolecules in the self-assembled structures, and show the unique versatility of dendritic macromolecules as molecular templates. Moreover, our previous study reported a novel supramolecular side-chain light-emitting copolymers containing different generations of dendritic electron-transporting proton-donors hydrogen-bonded (H-bonded) with proton-acceptor copolymers with both light-emitting and hole-transporting properties [11]. Especially, functionalized dendrimers with some mesogenic units may offer novel liquid crystalline (LC) properties, and thus to utilize such newly developed mesomorphic materials in a variety of applications [12–15]. Consequently,

* Corresponding author. Department of Materials Sci. and Eng., National Chiao Tung University, Hsinchu, Taiwan, ROC.
** Corresponding author. National Synchrotron Radiation Research Center, Hsinchu, 30076, Taiwan.
E-mail addresses: weitsung@nsrrc.org.tw (W.-T. Chuang), linhc@mail.nctu.edu.tw (H.-C. Lin).

https://doi.org/10.1016/j.polymer.2020.122880
Received 28 May 2020; Received in revised form 16 July 2020; Accepted 1 August 2020
Available online 14 August 2020
0032-3861/© 2020 Elsevier Ltd. All rights reserved.

supramolecular design to incorporate incompatible blocks of block copolymers with mesogenic dendrimers may be considered as the significant interest to form hierarchically self-assembled macromolecular materials. Interestingly, the associated mesomorphism with dendrimers can be finely tuned to generate various unique arrangements [16–19]. Specifically, liquid crystalline (LC) block copolymers, combining LC nano-phase order of the molecular level (around 1–10 nm) with long range ordered nano-scale domains (around 101–102 nm), provide a platform to explore the influence of the phase behavior of the LC block copolymers on the morphology. Thus, well designed LC block copolymers have been prepared for constructing advanced functional materials with complex structures and potential optical, electronic, or photo-responsive functionalities [20–27]. In addition, a LC block copolymer with brush-type architecture as a platform was developed for creating functional materials by magnetic-field directed self-assembly [28]. The mesogenic species, spacer length, monomer functionality, brush-chain length, and overall molecular weight were chosen and optimized to produce hexagonally packed cylindrical PLA domains which self-assemble and align parallel to an applied magnetic field by Kasi et al. As a result, these block copolymers elucidate the hierarchical packings of mesogens with respect to the morphological structures and the mesophasic transitions under various confinements [29–32].

Regarding the incorporation of dendritic ligands with block copolymers to obtain mesomorphic properties, only a few reports demonstrated the diversity of the ligands can be finely controlled to tune the morphologies and properties of the final complexes to generate well-ordered patterns [33–36]. Therefore, a series of polynorbornenes containing flexible and hydrophobic alkyl dendrons possessing the columnar nematic (ColN) LC phase were designed and synthesized by Jeong et al. [37]. By introducing a hydrophilic triethylene oxide linker and a rigid biphenyl mesogen on the dendron, a smectic A (SmA) LC phase was induced. This study reveals that the hierarchical superstructures of norbornene-based polymers can be precisely controlled by tuning the chemical structures and the physical interactions of side-chain pendants. The further incorporation of optical-switchable azobenzene mesogens into the denpols helps to construct finely tuned hierarchical superstructures with anisotropic physical properties and reversible photoisomerization [38]. Besides, the functionalized side-chains of block copolymers via noncovalent bonds have been also reported for the investigation of nanostructure-functionality correlation and the creation of particular nanostructures in functional block copolymers [39–41]. Hadjichristidis and Ruokolainen et al. showed that H-bonded LC side-chain diblock copolymers possess the lamellar morphology as two proton acceptor block copolymers containing two types of poly-(vinylpyridines) (i.e., block copolymers PBd-P2VP and PS-P4VP) mixed with a proton donor cholesteryl mesogen (CholHS) [42]. Moreover, Chen et al. report that the self-assembled supramolecular hexagonal columnar structures with tunable lattice sizes were constructed by mixing proton acceptor poly(4-vinylpyridine) (P4VP) H-bonded with different molar ratios of bent-core and linear mesogenic dendritic additives (from less than fully H-bonded up to fully H-bonded complexation). Similar to our dendritic pendant approach, they further developed a simple but effective strategy to tune the size of the columnar phase by building supramolecular copolymers with mixed bent-core and linear mesogenic dendritic pendants [43]. In general, the conventional linear supramolecular active blocks can be substituted with dendronized polymers to visualize the increased topological complexities and morphologies in contrast to the linear block copolymers. Importantly, the self-assembly behaviors of copolymers may be monitored by the balance of the driving forces, such as ordered packings of liquid crystalline blocks and the packing restriction effects originating from microphase-separated morphologies. The variations in the nature and compositions of block polymers provide effective approaches to manipulating mesomorphic behaviors and microphasic structures in liquid crystal polymers. Therefore, further investigations to discover more insights of the combination of block copolymers and dendritic liquid crystals for various associated applications are highly demanded.

The applications of supramolecular chemistry to involve self-assembled block copolymer systems enable the design of macromolecular architectures which are challenging to be achieved via conventional all-covalent routes. For instance, two outer blocks of supramolecular double-comb triblock terpolymers designed by Loos et al. [44] are able to interact with a surfactant via hydrogen bonding and thus to form a comb-shaped architecture upon complexation. While the neat triblock terpolymer only formed a triple lamellar morphology, multiple hierarchical structures in these supramolecular comb−coil−comb triblock terpolymers were constructed by simply adjusting the surfactant concentration. Furthermore, Schenning et al. [45] described a novel class of thermotropic liquid crystals (LCs) H-bonded with poly(4-vinylpyridine) homopolymer or poly(styrene)-b-poly(4-vinylpyridine) block copolymer (BCP) to acquire polymeric supramolecules were facilitated with glassy smectic and columnar sub-nanometer features. The hierarchical selfassembly afforded by the LC/BCP complexes further resulted in the vertical orientation of the LC features in thin films. Moreover, Chen et al. [46] report a simple but effective strategy to tune the size of the columnar phase by building liquid crystalline supramolecular copolymers with mixed dendritic side chains. They can precisely control the size of columnar structures in the nano-range by varying the grafting densities and the molar ratio of mixed side chains.

It is worth noting that dendritic supramolecular block-polymer complexes containing various generations of typical bent-core mesogens will become a series of liquid crystalline polymer to generate novel hierarchical self-assembled structures. Apart from conventional liquid crystalline polymers, high density bulky side groups of dendritic supramolecular block-polymer complexes are packed around the backbone and enforced to be somewhat stretched. Therefore, by varying the different generations of supramolecular dendritic proton donors and utilization of shear alignment driving forces in the block copolymers, it is possible to exert effective controls over the mesophasic properties and microphase structures, which are rarely mentioned in previous researches. Enlightened by our previous research results [47,48], we expanded various types (i.e., H-bonded linkage and terminal siloxane unit) along with the shape and confinement effects of the terminal siloxane groups on the self-assembled behavior of molecular arrangements in the H-bonded bent-core complexes to investigate the shape effects of the terminal siloxane groups on the self-assembled behavior of molecular arrangements, including the bilayer structures, which were controlled by the shape effects of the string- and cage-like siloxane termini. Herein, as shown in Chart 1 we report the construction of highly ordered hierarchically self-assembled macromolecular materials by utilizing the triblock copolymer (i.e., **VSV**) and two generations of dentritic bent-core mesogenic pendants (i.e., **G1** and **G2**), which were performed to functionalize side-chains with bent-core mesogenic dendrimers via noncovalent bonds (H-bonds). Interestingly, the hierarchical H-bonded structures were further utilized to construct functionalized self-assemblies of triblock copolymer **VSV** in supramolecular polymer complexes (i.e., **VSV/G1** and **VSV/G2**) via the sheared alignment of various generations of dentritic bent-core smectogens.

2. Experimental

2.1. Synthetic procedures

The synthetic routes of compounds **A12** and **V–OH** are shown in Scheme 1. In addition, the synthetic routes of mesogenic dendritic proton donors **G1** and **G2** are shown in Scheme 2. The detailed synthetic procedures and chemical characterization of all compounds are described in the supporting information [49–51].

Reagents and conditions: (a) CH_2Cl_2, r.t., overnight; (b) K_2CO_3, KI, acetone, reflux, 48 h (c) (i) *n*-BuLi, THF, −78 °C, (ii) triisopropyl borate, (iii) 10% HCl; (d) $Pd(PPh_3)_4$, K_2CO_3, EtOH/toluene (1:3, v/v), 90 °C, 5 h; (e) DCC, DMAP, CH_2Cl_2, r.t., 16 h; (f) H_2, 10% Pd–C, THF; (g) HBr (48%

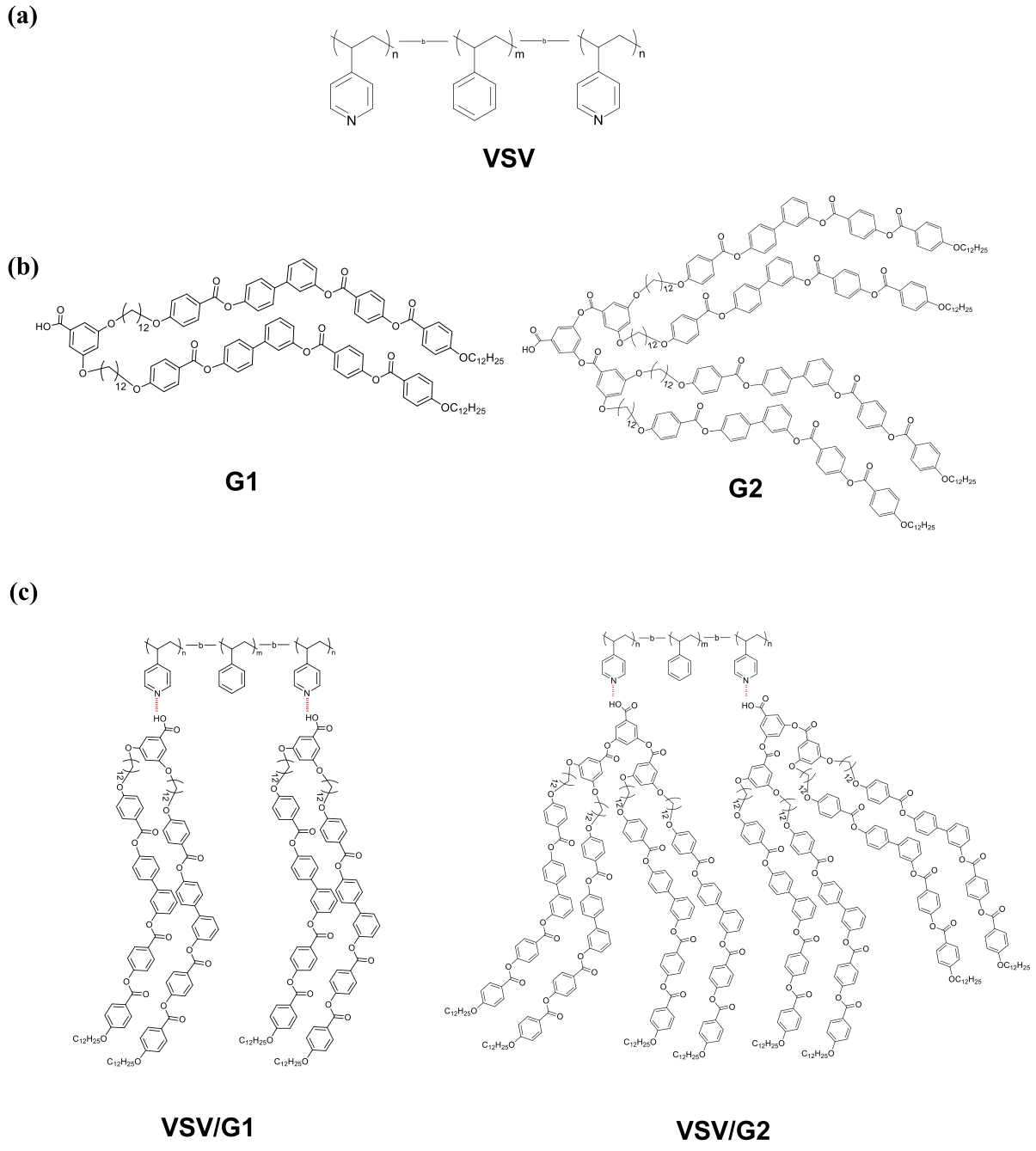

Chart 1. Chemical structures of (a) triblock copolymer proton acceptor poly(4-vinylpyridine)-block-polystyrene-block-poly(4-vinylpyridine) (**VSV**), (b) mesogenic dendritic proton donors **G1** and **G2**, and (c) supramolecular LC block copolymer complexes **VSV/G1** and **VSV/G2**, where the molecular weight distribution of **VSV** is Mn = P4VP(4500)-PS(27000)-P4VP(4500).

in water), toluene, reflux; (h) PPTS, CH_2Cl_2, r.t., overnight; (i) KOH, EtOH, reflux, overnight, then NH_4Cl aqueous; (j) PTSA, CH_2Cl_2/MeOH (3:1, v/v), 50 °C, overnight.

2.2. Preparation of complexes *VSV/G1* and *VSV/G2*

These supramolecular LC block copolymer complexes (i.e., **VSV/G1** and **VSV/G2**) are composed of a triblock copolymer (**VSV**) as a proton acceptor and two generations of dentritic pendants (**G1** and **G2**) as proton donors, where **VSV** possesses the molecular weight distribution of Mn = P4VP(4500)-PS(27000)-P4VP(4500). The block copolymer **VSV** and two generations of dentritic pendants (**G1** and **G2**) were mixed with the molar ratio of 100% fully H-bonded to each other in both supramolecular LC block copolymer complexes (i.e., **VSV/G1** and **VSV/G2**), which were dissolved separately in tetrahydrofuran (THF) to form clear solutions with the concentration of 5 wt%. The complexes were then prepared by mixing appropriate amounts of the two solutions, and the THF solvent was removed to be evaporated slowly at 60 °C for 24 h. Finally, the samples were dried under vacuum at 100 °C for 24 h to remove the residual solvent. All the complexes were further annealed at 120 °C for 48 h to enhance the long-range order of the supramolecular LC block copolymer complexes.

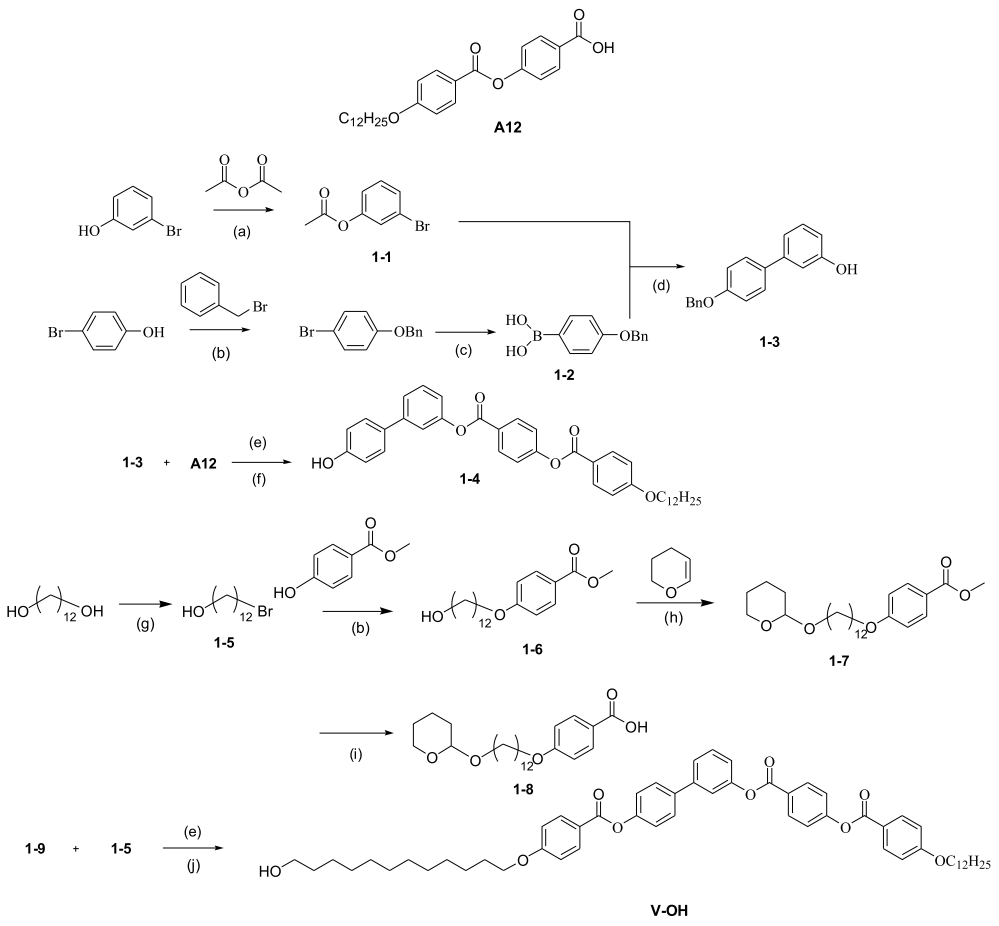

Scheme 1. Synthetic route of **V–OH**.

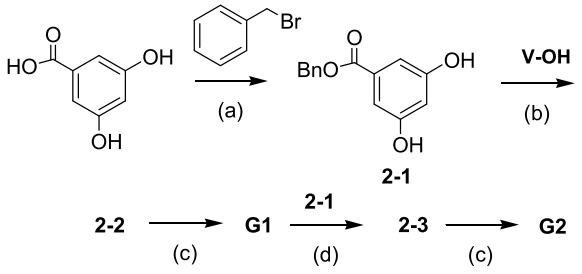

Scheme 2. Synthetic route of mesogenic dendritic proton donors **G1** and **G2**.

2.3. Characterization methods

^{1}H NMR spectra were recorded using a Bruker Advance 300 MHz spectrometer, with DMSO-d_6 and $CDCl_3$ as solvents. Mass spectral data were obtained using a Micromass TRIO-2000 GC/MS system. Elemental analyses were performed using a Heraeus CHN-OS RAPID elemental analyzer. The optical textures were observed using a polarizing optical microscopy (POM) Leica DMLP equipped with a Linkam hot stage. Transmission electron microscopy (TEM) images were obtained on a JEOL JEM2100 microscope with an accelerating voltage of 200 kV. The solvent-casted block copolymers were annealed in chloroform for 12 h, the ultrathin sections of P4VP were stained with I_3^- in triblock copolymer (**VSV**) to enhance contrast for TEM images. Differential scanning calorimetry (DSC) experiments were conducted using a Mettler Toledo DSC822e/400 connected with liquid nitrogen cooler. Synchrotron-based small-angle and wide-angle X-ray scattering measurements in conjunction with grazing-incidence scattering (SAXS/GISAXS and WAXS/GIWAXS, respectively) were performed at the BL23A1 SAXS and BL17A1 XRD end stations, respectively, of the National Synchrotron Radiation Research Center, Hsinchu, Taiwan [51]. With the marCCD165 detector used for SAXS and the mar345 image plate for WAXS, typical scattering patterns were collected from at least 60–300 s to obtain sufficient scattering intensities. The beam diameter of the 10 keV beam (λ = 0.124 nm) was 0.5 mm. The scattering vectors ($q = 4\pi/\lambda \sin\theta$; with scattering angle 2θ) for SAXS and WAXS were calibrated using two standard samples of silver behenate and silicon.

3. Results and discussion

Herein, the hierarchical H-bonded structures were performed to functionalize side-chains with mesogenic dendrimers via noncovalent bonds (H-bonds) to construct functionalized self-assemblies. Thus, a series of supramolecular LC block copolymer complexes (i.e., **VSV/G1** and **VSV/G2**) containing one triblock copolymer proton acceptor, i.e., poly(4-vinylpyridine)-block-polystyrene-block-poly(4-vinylpyridine) (**VSV** in Chart 1a, i.e., P4VP-PS-P4VP), hydrogen-bonded (H-bonded) with two generations of mesogenic dendritic proton donors (**G1** and **G2** in Chart 1b) were developed in this research as shown in Chart 1c. The phase behavior and self-assembled patterns of supramolecular polymer complexes **VSV/G1** and **VSV/G2**, which contain triblock copolymer proton acceptor **VSV** complexed with mesogenic dendritic proton donors **G1** and **G2**, have been characterized by differential scanning calorimetry (DSC), wide- and small-angle X-ray scattering (WAXS and SAXS) and transmission electron microscopy (TEM). The mesophasic behavior and transition temperatures of mesogenic dendritic proton donors (**G1** and **G2**) and their respective supramolecular polymer complexes **VSV/G1** and **VSV/G2** are displayed in Table 1. The polarized

optical microscopy (POM) photos and DSC data of dendritic proton donors **G1** and **G2** are illustrated in Figs. S3 and S4. Both proton donors **G1** and **G2** exhibited smectic A (SmA) phase, which was originated from the mesogenic nature of the bent-core structure in dendritic proton donors (**G1** and **G2**) and their XRD results will further verify the smectic layer arrangement. As cooled down below the SmA phase range (up to room temperature), an unidentified smectic X (SmX) phase with small phase transition enthalpy changes was observed in dendritic proton donors (**G1** and **G2**), where the layer arrangement of SmX for **G1** and **G2** was later confirmed by XRD measurements (as shown in Fig. S6).

Moreover, **G1** possessed wider mesophasic range (44.8 °C) and higher isotropization temperature (99.3 °C) than **G2** (30.0 °C and 76.3 °C, respectively), which is due to the less constrain of self-assembled behavior in the lower generation of **G1** (with two bent-core dendritic arms and less branches) in contrast to **G2** (with four bent-core dendritic arms and more branches). After blending dendritic proton donors (**G1** and **G2**) with triblock copolymer proton acceptor **VSV**, both of their respective supramolecular polymer complexes **VSV/G1** and **VSV/G2** possessed the SmA phase (but without the SmX phase). Accordingly, the isotropization temperatures of supramolecular polymer complexes **VSV/G1** and **VSV/G2** are 107.7 °C and 97.8 °C, respectively, which followed the same trend of proton donors **G1** and **G2**, i.e. **VSV/G1** > **VSV/G2**. In addition, due to the higher molecular weights of supramolecular polymer complexes the isotropization temperatures of supramolecular polymer complexes **VSV/G1** and **VSV/G2** are higher than their respective proton donors **G1** and **G2**, i.e. **VSV/G1** (107.7 °C) > **G1** (99.3 °C) and **VSV/G2** (97.8 °C) > **G2** (76.3 °C).

The results of wide- and small-angle X-ray scattering (WAXS and SAXS) measurements are compared to analyze the molecular packings in their self-assembled arrangements of the dendritic proton donors (**G1** and **G2**), triblock copolymer proton acceptor **VSV** and their respective supramolecular polymer complexes **VSV/G1** and **VSV/G2**. As shown in Fig. S6, the d-spacing values 8.12 nm ($q = 0.773\ nm^{-1}$) and 7.82 nm ($q = 0.803\ nm^{-1}$) of **G1** and **G2** in their mesophasic range exhibited an interdigitated layer structure to further confirm the smectic A phase, where the theoretical molecular chain lengths of **G1** and **G2** are 5.96 nm and 6.44 nm, respectively, were the simulated results calculated by using PM3. Moreover, the d-spacing values of **VSV/G1** and **VSV/G2** in Fig. S6 are 6.46 nm ($q = 0.972\ nm^{-1}$) and 8.28 nm ($q = 0.758\ nm^{-1}$), which also showed the smectic A phase with an interdigitated layer structure in the liquid crystalline state.

The two-dimensional small-angle X-ray scattering (SAXS) patterns, diffractograms, and molecular arrangements of the mesogenic dendritic proton donors (**G1** and **G2**) and supramolecular polymer complexes **VSV/G1** and **VSV/G2** after shear treatments [45,52,53], which induced better alignments to observe the self-assembled morphologies of block copolymers, and quenched at their mesophasic temperatures are illustrated in Figs. 1–4, respectively. Moreover, the TEM images and structural models of both mesogenic supramolecular polymer complexes **VSV/G1** and **VSV/G2** after shear alignment and quenched at their mesophasic temperatures are also demonstrated in Figs. 3 and 4, respectively. The molecular structures of the mesogenic dendritic proton donors **G1** and **G2** simulated by PM3 are revealed in Fig. S7. Thus, according to the SAXS results and simulation of PM3, the possible schematic representations of **G1** and **G2** in their liquid-crystalline structures are shown in Figs. 1c and 2c, respectively. Finally, simplified 3D-order structural models for the possible molecular arrangements of both supramolecular polymer complexes **VSV/G1** and **VSV/G2** were analyzed by further TEM images along with SAXS results.

Table 1
Phase behaviour of mesogenic dendritic proton donors (**G1** and **G2**) and supramolecular polymer complexes **VSV/G1** and **VSV/G2** determined by DSC.

Compound	Phase transition/°C (Enthalpy/J/g) [a]
G1	**ISO** [b] 99.3 (-24.2) **SmA** 54.5 (-0.8) **SmX** [c]
G2	**ISO** 76.3 (-8.9) **SmA** 46.3 (-1.5) **SmX** [c]
VSV/G1 [d]	**ISO** 107.7 (-7.5) **SmA**
VSV/G2 [d]	**ISO** 97.8 (-2.8) **SmA**

[a] Data show the second cooling of DSC thermograms.
[b] **ISO**: isotropic state, **SmA**: smectic A phase. **SmX**: smectic X phase.
[c] The layer arrangement of SmX for **G1** and **G2** is confirmed by XRD measurements.
[d] Glass transition temperature of **VSV** is 121.3 °C with an enthalpy of 0.9 J/g and its DSC data are illustrated in Fig. S5.

As shown in Fig. 1a and b, the scattering vectors of three scattering peaks in dendritic proton donors **G1** are observed at $q = 0.77\ nm^{-1}$, $1.60\ nm^{-1}$, and $2.31\ nm^{-1}$ with a ratio of 1: 2: 3, which was indicative of a lamellar structure of the smectic A phase with a repeating distance (d-spacing) of 8.15 nm. Similarly, the scattering vectors of $q = 0.81\ nm^{-1}$, $1.62\ nm^{-1}$, and $2.43\ nm^{-1}$ (with a ratio of 1: 2: 3) are acquired in Fig. 2a and b to feature a lamellar structure in dendritic proton donors **G2** with a repeating distance (d-spacing) of 7.75 nm. According to the theoretical model (PM3) of **G1** and **G2** in Fig. S7, their molecular lengths can be calculated as 5.96 nm and 6.44 nm, respectively. With the previous molecular lengths simulated by PM3 and d-spacing results of SAXS, the possible smectic A schematic representations of hierarchical structural arrangements for **G1** and **G2** are suggested to have the interdigitated layer structure with head-to-head and end-overlapping conformations of bent-core liquid crystals in Figs. 1c and 2c, respectively. Before complexation, the two-dimensional small-angle X-ray scattering (2D SAXS) pattern and diffractogram of triblock copolymer proton acceptor **VSV** in Fig. S8 are utilized to examine the self-assembled structures of H-bonded acceptor **VSV**. Compared with the lamellar structure of dendritic proton donors **G1** and **G2**, the main chains of triblock copolymer proton acceptor (**VSV**) exhibits only two sharp peaks ($q = 0.097\ nm^{-1}$ and $0.269\ nm^{-1}$) in the SAXS diffractogram of Fig. S8b, which suggests a less order stacking in three-dimensional structure. Regarding supramolecular polymer complex **VSV/G1**, its two-dimensional SAXS pattern and diffractogram possess the first set of scattering peaks with a q/q1 ratio of 1:2:3 (green) in Fig. 3a and b, indicating the formation of a lamellar (LC interdigitated layer) structure of the Sm A phase. Moreover, the second set of scattering peaks with a q/q1 ratio of $1:\sqrt{2}:\sqrt{5}$ (violet) suggests the formation of a tetragonal structure (i.e., P4VP core of dendron-jacketed (P4VP/**G1**) columnar domains) with a columnar distance of 6.6 nm (calculated from $q = 0.952\ nm^{-1}$ of the lamellar structure between P4VP layers). Furthermore, the third set of scattering peaks with a q/q1 ratio of $1:\sqrt{3}:\sqrt{9}$ (red) in the smallest q region demonstrates a BCC structure with microphase-spearated PS domains. In addition, the BCC phase was also confirmed by the TEM bright-field image (Fig. 3c) along the [100] direction, where P4VP stained with I_3^- are in the matrix and the polystyrene chain cages form the spherical cores on corners. As the minor domain in its periodical length of PS, the calculated d-spacing value of 26.97 nm (i.e., d-spacing $= 2\pi/q$) in the BCC phase of Fig. 3d is obtained from $q = 0.233\ nm^{-1}$ in the smallest q region of Fig. 3b, which gives rise to the matchable result of an experimentally acquired d-spacing value of 27.36 nm in the inset of the TEM image (Fig. 3c). Importantly, a novel hierarchical lamellar-*within*-tetragonal-*within*-BCC structure in Fig. 3d is accordingly verified by the TEM moropholgy of complex **VSV/G1**, which was rarely found in the literature [52].

Similarly, the SAXS 2D pattern and diffractogram of supramolecular polymer complex **VSV/G2** in Fig. 4a and b shows the first set of scattering peaks with a q/q1 ratio of 1:2:3 (green) in Fig. 4a and b, indicating the formation of a lamellar (LC interdigitated layer) structure of the Sm A phase. Moreover, the second set of scattering peaks with a q/q1 ratio of $1:\sqrt{3}:\sqrt{7}$ (violet) suggests the formation of a hexagonal structure (i.e., P4VP core of dendron-jacketed (P4VP/**G2**) columnar domains) with a columnar distance of 8.41 nm (calculated from $q = 0.747\ nm^{-1}$ of the lamellar structure between P4VP layers). Furthermore, the third set of scattering peaks with a q/q1 ratio of $1:\sqrt{(8/3)}:\sqrt{(16/3)}$ (red) in the smallest q region demonstrates a face-centered cubic packing (i.e., a FCC structure) with microphase-spearated PS domains. In addition, the FCC phase was also confirmed by the TEM bright-field image (Fig. 4c) along

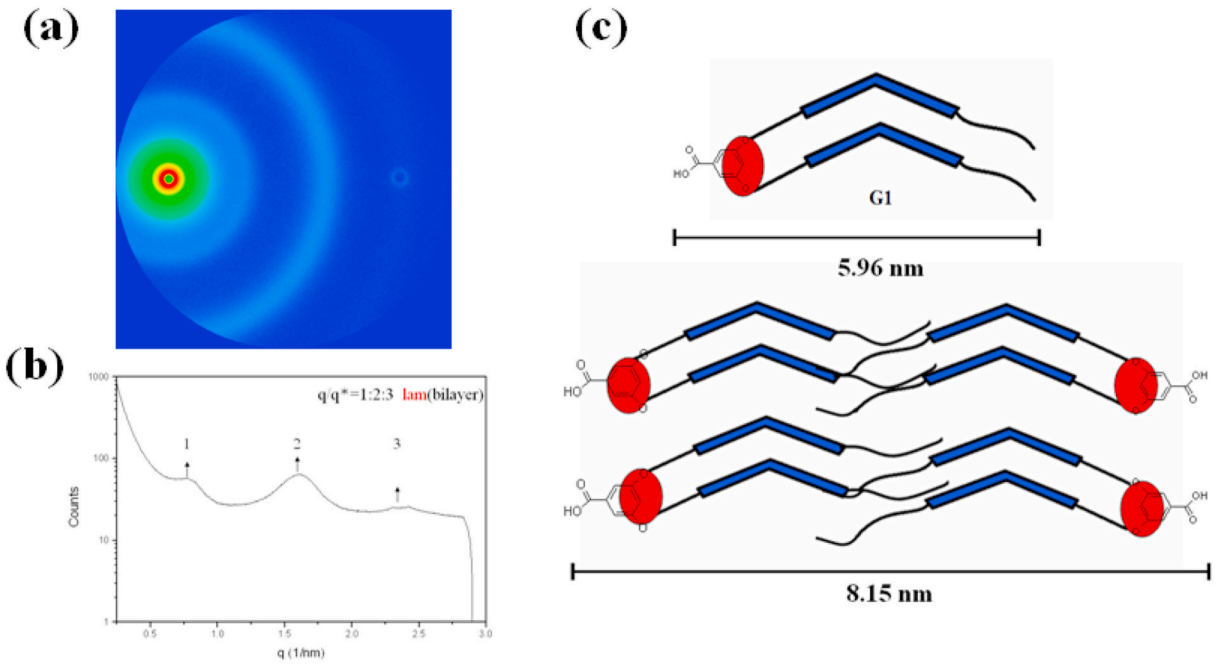

Fig. 1. (a) 2D SAXS pattern and (b) diffractogram of mesogenic dendritic proton donor **G1** after shear alignment and quenched at the mesophasic temperature, (c) schematic representation of hierarchical structural arrangements for dendrimer **G1.**

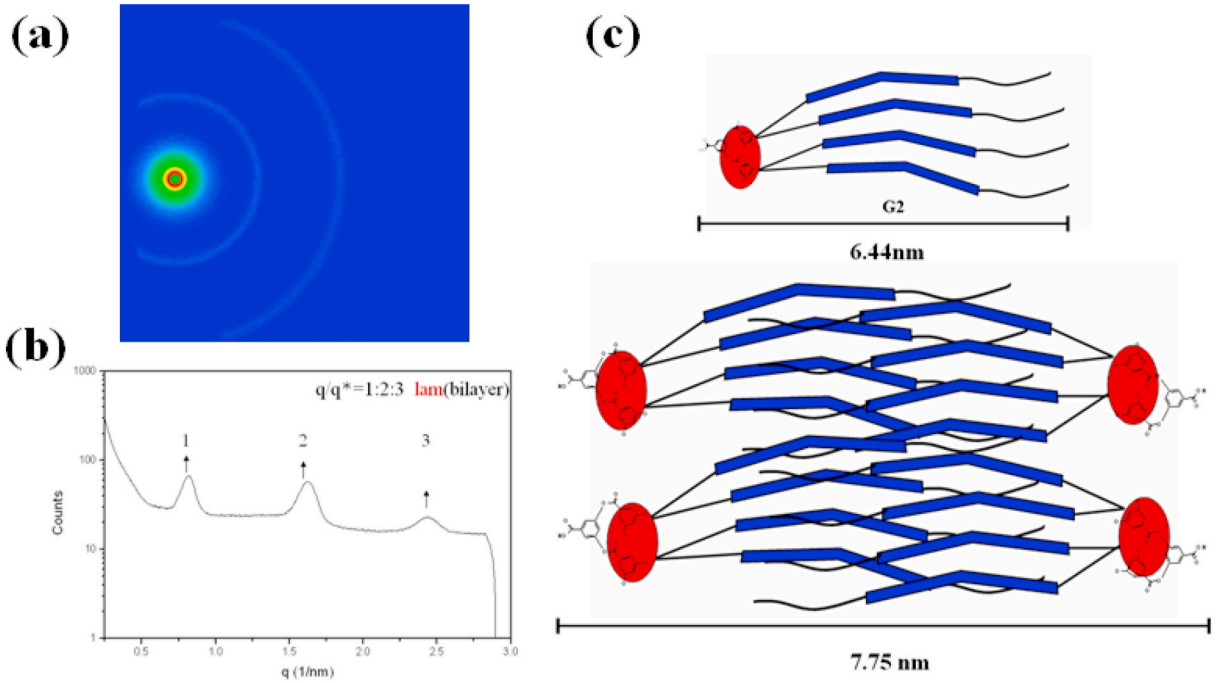

Fig. 2. (a) 2D SAXS pattern and (b) diffractogram of mesogenic dendritic proton donor **G2** after shear alignment and quenched at the mesophasic temperature. (c) Schematic representation of hierarchical structural arrangements for dendrimer **G2**.

the [100] direction, where P4VP are in the matrix and the polystyrene chain cages form the spherical cores on corners. As the minor domain in its periodical length of PS, the calculated d-spacing value of 27.32 nm (i.e., d-spacing = $2\pi/q$) in the BCC phase of Fig. 4d is obtained from q = 0.230 nm^{-1} in the smallest q region of Fig. 4b, which gives rise to the matchable result of an experimentally acquired d-spacing value of 27.71 nm in the inset of the TEM image (Fig. 4c) by staining P4VP with I_3^-. Prominently, a novel hierarchical lamellar-*within*-hexagonal-*within*-FCC structure in Fig. 4d is consequently verified by the TEM morophology of complex **VSV/G2**, which was also seldom reported even for block-copolymers. According to the investigated results of 2D SAXS patterns and TEM morphologies, supramolecular polymer complexes **VSV/G1** and **VSV/G2** were observed to possess different hierarchical lamellar domains of bent-core dendritic proton donors (**G1** and **G2**) organized in corresponding tetragonal and hexagonal arrangements, and thereafter were H-bonded with triblock copolymer proton acceptor **VSV** and self-assembled to result in BCC and FCC structures, respectively.

In this study, the SAXS results indicate that two generations of

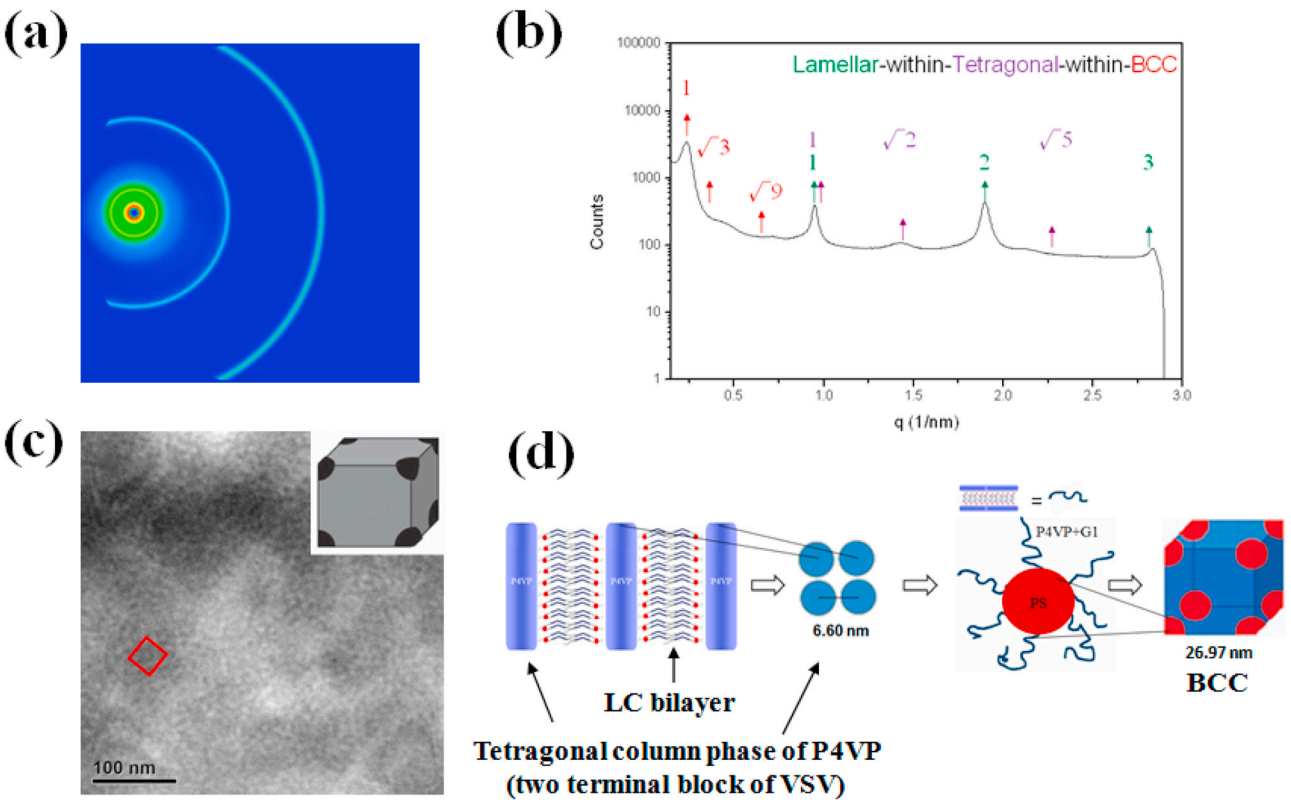

Fig. 3. (a) 2D SAXS pattern and (b) diffractogram of supramolecular polymer complex **VSV/G1** after shear alignment and quenched at the mesophasic temperature. (c) TEM image for complex **VSV/G1**. (d) A simplified 3D-order BCC structural model of the possible molecular arrangements.

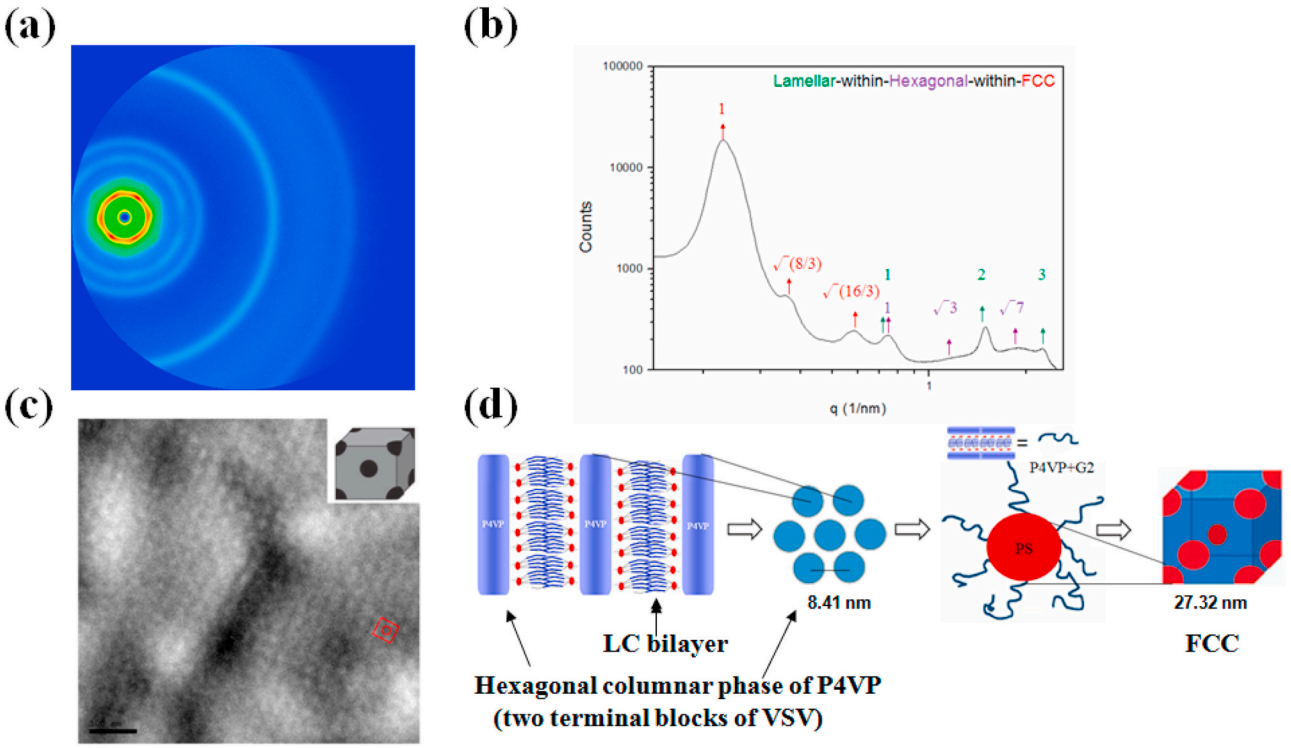

Fig. 4. (a) 2D SAXS pattern and (b) diffractogram of supramolecular polymer complex **VSV/G2** after shear alignment and quenched at the mesophasic temperature. (c) TEM image for complex **VSV/G2**. (d) A simplified 3D-order FCC structural model of the possible molecular arrangements.

dendritic proton donors (**G1** and **G2**) can be self-assembled into a hierarchically ordered lamellar structure with two different layer thicknesses. The LC molecules are aligned into head-to-head layered arrangement and form a layer structure between the polymer backbones, which dominate the highly ordered LC phase and allow side-chains with H-bonded mesogenic dendrimers to pack inside with their axes perpendicular to those backbones and to form a smectic packing above their mesophasic temperatures. While the backbones of triblock copolymer (proton acceptor **VSV**) greatly inhibit the motion of the side-chain mesogens, which can be achieved using a shear alignment force in the smectic phase to induce the movements of main chains and side chains cooperatively. Further construction of supramolecular polymer complexes **VSV/G1** and **VSV/G2** with different 3D positional order in nanometer scale. Experimental and theoretical studies well demonstrated our new approach to generate the LC triblock copolymers based hierarchical self-assemblies, where conventional linear side-chains on supramolecular active blocks were substituted with two generations of our dendritic side-chains to visualize the increased topological complexities and morphologies in contrast to the linear block copolymer proton donor where such findings are absent in the literature. Importantly, the self-assembled behavior of copolymers have been monitored by the shear alignment driving forces, such as ordered packing of liquid crystalline blocks and the packing restriction effect originated from microphase-separated morphologies. The combination of the nature and composition of block polymers with various generations of our dendritic bent-core mesogens provides an effective approach to manipulate the mesomorphic behavior and the 3D-order microphasic structures in these novel supramolecular liquid crystal polymers.

4. Conclusions

In conclusion, a series of side-chain supramolecular polymer complexes **VSV/G1** and **VSV/G2** based on H-bonded interactions between proton acceptor triblock copolymer **VSV** and two generations of proton donor bent-core mesogenic dendritic pendants (**G1** and **G2**) were prepared and investigated. Significant hierarchical self-assemblies generated by the increased topological complexities have been well studied and explored by the wide- and small-angle X-ray scattering (WAXS and SAXS) experiments, polarized optical microscopy (POM), differential scanning calorimetry (DSC) and transmission electron microscopy (TEM). Based on the experimental and theoretical studies of 2D SAXS patterns, diffractograms and TEM morphologies, our new approaches of supramolecular polymer complexes **VSV/G1** and **VSV/G2** well demonstrate that the introduction and manipulation of novel hierarchical lamellar-within-tetragonal(or hexagonal)-within-BCC (or FCC) structures were dominated by the self-assemblies of different generations of H-bonded dendritic proton donors (**G1** and **G2**) and triblock copolymer proton acceptor **VSV**. Hence, our experimental results demonstrate that the localized layered structure in small domains correspond to the smectic arrangements of the pendent dendrimers and the characteristic structures in large domains match the BCC and FCC scales of their respective blocks. Thus, these supramolecular systems may offer new possibilities in the design of hierarchical self-assembled polymeric materials as templates to be combined with their complementary dendritic mesogenic moieties for future applications.

CRediT authorship contribution statement

Chien-Min Lin: Data curation, Formal analysis, Investigation, Methodology, Validation, Visualization, Roles/Writing - original draft, Writing - review & editing. **Atul Kumar Dwivedi:** Data curation, Formal analysis, Investigation, Methodology, Validation, Visualization, Roles/Writing - original draft, Writing - review & editing. **Wei-Tsung Chuang:** Conceptualization, Funding acquisition, Data curation, Formal analysis, Project administration, Resources, Supervision, Investigation, Methodology, Validation, Visualization, Roles/Writing - original draft, Writing - review & editing. **Hong-Cheu Lin:** Conceptualization, Funding acquisition, Data curation, Formal analysis, Project administration, Resources, Supervision, Investigation, Methodology, Validation, Visualization, Roles/Writing - original draft, Writing - review & editing.

Declaration of competing interest

The authors declare that they have no known competing financial interests or personal relationships that could have appeared to influence the work reported in this paper.

Acknowledgements

The authors are grateful for funding from the Ministry of Science and Technology, Taiwan (grant No. MOST106-2113-*M*-009-012-MY3, 107-2221-E-009-043-MY2 and 108-3017-F-009-004) and the Center for Emergent Functional Matter Science of National Chiao Tung University from The Featured Areas Research Center Program within the framework of the Higher Education Sprout Project by the Ministry of Education (MOE) in Taiwan.

Appendix A. Supplementary data

Supplementary data to this article can be found online at https://doi.org/10.1016/j.polymer.2020.122880.

References

[1] S.A. Jenekhe, X.L. Chen, Science 283 (1999) 372–375.
[2] E. Kim, S. Park, Y.S. Han, T.H. Kim, Polymer 150 (2018) 214–222.
[3] S. Park, Polymer 180 (2019), 121726.
[4] I.O. Lebedeva, E.B. Zhulina, O.V. Borisov, Macromolecules 52 (2019) 3655–3667.
[5] H. Noh, S. Myung, M.J. Kim, S.K. Yang, Polymer 175 (2019) 65–70.
[6] S. Ahn, J. Nam, J. Zhu, E. Lee, S.M. Kilbey, Polym. Chem. 9 (2018) 3279–3286.
[7] Z. Sun, X. Li, G. Zhu, L. Xue, Y. Zhou, Z. Yi, C. Gao, Polymer 156 (2018) 240–249.
[8] H. Li, J. Wu, J.F. Yin, H. Wang, Y. Wu, G.C. Kuang, Macromol. Rapid Commun. 40 (2019) 1800714.
[9] L.M. Pitet, B.M. Chamberlain, A.W. Hauser, M.A. Hillmyer, Polym. Chem. 10 (2019) 5385–5395.
[10]] A.J. Soininen, E. Kasemi, A.D. Schluter, O. Ikkala, J. Ruokolainen, R. Mezzenga, J. Am. Chem. Soc. 132 (2010) 10882–10890.
[11] P.J. Yang, C.W. Wu, D. Sahu, H.C. Lin, Macromolecules 41 (2008) 9692–9703.
[12] Y. Chen, S. Huang, T. Wang, Z. Dong, H. Yu, Macromolecules 52 (2019) 1892–1898.
[13] W. Wen, T. Huang, S. Guan, Y. Zhao, A. Chen, Macromolecules 52 (2019) 2956–2964.
[14] J. Jin, M. Tang, Z. Zhang, K. Zhou, Y. Gao, Z.G. Zheng, W. Zhang, Polym. Chem. 9 (2018) 2101–2108.
[15] M. Gopinadhan, Y. Choo, C.O. Osuji, ACS Macro Lett. 5 (2016) 292–296.
[16] K. Deepthi, R.R.B. Amal, V.R. Rajeev, K.N.N. Unni, E.B. Gowd, Macromolecules 52 (2019) 2889–2899.
[17] S.J. Dalsin, T.G. Rions-Maehren, M.D. Beam, F.S. Bates, M.A. Hillmyer, M. W. Matsen, ACS Nano 9 (2015) 12233–12245.
[18] H. Pan, A. Xiao, W. Zhang, L. Luo, Z. Shen, X. Fan, Polymer 182 (2019) 121835.
[19] W. Wagner, M. Wehner, V. Stepanenko, F. Würthner, J. Am. Chem. Soc. 141 (2019) 12044–12054.
[20] S.I. Stupp, V. LeBonheur, K. Walker, L.S. Li, K.E. Huggins, M. Keser, A. Amstutz, Science 276 (1997) 384–389.
[21] K.K. Tenneti, X. Chen, C.Y. Li, Y. Tu, X. Wan, Q.-F. Zhou, I. Sics, B.S. Hsiao, J. Am. Chem. Soc. 127 (2005) 15481–15490.
[22] K. Nickmans, R.C.P. Verpaalen, J.N. Murphy, A.P.H.J. Schenning, J. Mater. Chem. C 6 (2018) 3042–3046.
[23] D. Wang, G. Ye, Y. Zhu, X. Wang, Macromolecules 42 (2009) 2651–2657.
[24] J.G. Son, X. Bulliard, H. Kang, P.F. Nealey, K. Char, Adv. Mater. 20 (2008) 3643–3648.
[25] G. Gobius du Sart, I. Vukovic, G.A. van Ekenstein, E. Polushkin, K. Loos, G. Ten Brinke, Macromolecules 43 (2010) 2970–2980.
[26] Y. Choo, L.H. Mahajan, M. Gopinadhan, D. Ndaya, P. Deshmukh, R.M. Kasi, C. O. Osuji, Macromolecules 48 (2015) 8315–8322.
[27] M. Gopinadhan, P. Deshmukh, Y. Choo, P.W. Majewski, O. Bakajin, M. Elimelech, R.M. Kasi, C.O. Osuji, Adv. Mater. 26 (2014) 5148–5154.
[28] P. Deshmukh, M. Gopinadhan, Y. Choo, S.K. Ahn, P.W. Majewski, S.Y. Yoon, O. Bakajin, M. Elimelech, C.O. Osuji, R.M. Kasi, ACS Macro Lett. 3 (2014) 462–466.
[29] J. Korhonen, T.T. Verho, P. Rannou, O. Ikkala, Macromolecules 43 (2010) 1507–1514.
[30] S.P. Nunes, R. Sougrat, B. Hooghan, D.H. Anjum, A.R. Behzad, L. Zhao, N. Pradeep, I. Pinnau, U. Vainio, K.V. Peinemann, Macromolecules 43 (2010) 8079–8085.

[31] M. Gopinadhan, E.S. Beach, P.T. Anastas, C.O. Osuji, Macromolecules 43 (2010) 6646–6654.
[32] C. Tang, W. Wu, D.-M. Smilgies, K. Matyjaszewski, T. Kowalewski, J. Am. Chem. Soc. 133 (2011) 11802–11809.
[33] W.B. Lee, R. Elliott, R. Mezzenga, G.H. Fredrickson, Macromolecules 42 (2009) 849–859.
[34] M.R. Hammond, R. Mezzenga, Soft Matter 4 (2008) 952–961.
[35] C. Li, A.D. Schluter, A. Zhang, R.A. Mezzenga, Adv. Mater. 20 (2008) 4530–4534.
[36] B.M. Rosen, C.J. Wilson, D.A. Wilson, M. Peterca, M.R. Imam, V. Percec, Chem. Rev. 109 (2009) 6275–6540.
[37] D.Y. Kim, D.G. Kang, S. Shin, T.L. Choi, K.U. Jeong, Polym. Chem. 7 (2016) 5304–5311.
[38] D.Y. Kim, S. Shin, W.J. Yoon, Y.J. Choi, J.K. Hwang, J.S. Kim, C.R. Lee, T.L. Choi, K.U. Jeong, Adv. Funct. Mater. 27 (2017), 1606294.
[39] J.J. Miao, L.H. Cui, P. Lau, P.T. Mather, L. Zhu, Macromolecules 40 (2007) 5460–5470.
[40] D. Ndaya, R. Bosire, L. Mahajan, S. Huh, R. Kasi, Polym. Chem. 9 (2018) 1404–1411.
[41] A.H. Hofman, M. Reza, J. Ruokolainen, G. Brinke, K. Loos, Macromol. Rapid Commun. 38 (2017) 1700288.
[42] A.J. Soininen, I. Tanionou, N. Brummelhuis, H. Schlaad, N. Hadjichristidis, O. Ikkala, J. Raula, R. Mezzenga, J. Ruokolainen, Macromolecules 45 (2012) 7091–7097.
[43] Y. Cai, M. Zheng, Y. Zhu, X.F. Chen, C.Y. Li, ACS Macro Lett. 6 (2017) 479–484.
[44] A.H. Hofman, I. Terzic, M.C.A. Stuart, G. Brinke, K. Loos, ACS Macro Lett. 7 (2018) 1168–1173.
[45] K. Nickmans, R.C.P. Verpaalen, J.N. Murphy, A.P.H.J. Schenning, J. Mater. Chem. C 6 (2018) 3042–3046.
[46] Y. Cai, M. Zheng, Y. Zhu, X.F. Chen, C.Y. Li, ACS Macro Lett. 6 (2017) 479–484.
[47] W.H. Chen, W.T. Chuang, U.S. Jeng, H.S. Sheu, H.C. Lin, J. Am. Chem. Soc. 133 (2011) 15674–15685.
[48] I.H. Chiang, W.T. Chuang, C.L. Lu, M.T. Lee, H.C. Lin, Chem. Mater. 27 (2015) 4525–4537.
[49] C. Cativiela, J.L. Serrano, M.M. Zurbano, J. Org. Chem. 60 (1995) 3074–3083.
[50] D. Shen, A. Pegenau, S. Diele, I. Wirth, C. Tschierske, J. Am. Chem. Soc. 122 (2000) 1593–1601.
[51] U.S. Jeng, J. Appl. Crystallogr. 43 (2010) 110–121.
[52] W.T. Chuang, H.S. Sheu, U.S. Jeng, H.H. Wu, P.D. Hong, J.J. Lee, Chem. Mater. 21 (2009) 975–978.
[53] J.B. Jheng, W.T. Chuang, P.D. Hong, Y.C. Huang, U.S. Jeng, C.J. Su, G.R. Pan, Polymer 54 (2013) 6242–6252.